Proceedings of ASME Turbo Expo 2019: Turbomachinery Technical Conference and Exposition
SAND2019-1762C
GT2019
June 17-21, 2019, Phoenix, Arizona, USA

GT2019-90493

SCO2 POWER CYCLE COMPONENT COST CORRELATIONS FROM DOE DATA SPANNING MULTIPLE SCALES AND APPLICATIONS

Nathan T. Weiland
National Energy Technology Laboratory
Pittsburgh, PA, USA

Blake W. Lance
Sandia National Laboratories
Albuquerque, NM, USA

Sandeep R. Pidaparti
National Energy Technology Laboratory
KeyLogic
Pittsburgh, PA, USA

ABSTRACT

Supercritical CO_2 (sCO_2) power cycles find potential application with a variety of heat sources including nuclear, concentrated solar (CSP), coal, natural gas, and waste heat sources, and consequently cover a wide range of scales. Most studies to date have focused on the performance of sCO_2 power cycles, while economic analyses have been less prevalent, due in large part to the relative scarcity of reliable cost estimates for sCO_2 power cycle components. Further, the accuracy of existing sCO_2 techno-economic analyses suffer from a small sample set of vendor-based component costs for any given study. Improved accuracy of sCO_2 component cost estimation is desired to enable a shift in focus from plant efficiency to economics as a driver for commercialization of sCO_2 technology.

This study reports on sCO_2 component cost scaling relationships that have been developed collaboratively from an aggregate set of vendor quotes, cost estimates, and published literature. As one of the world's largest supporters of sCO_2 research and development, the Department of Energy (DOE) National Laboratories have access to a considerable pool of vendor component costs that span multiple applications specific to each National Laboratory's mission, including fossil-fueled sCO_2 applications at the National Energy Technology Laboratory (NETL), CSP at the National Renewable Energy Laboratory (NREL), and CSP, nuclear, and distributed energy sources at Sandia National Laboratories (SNL). The resulting cost correlations are relevant to sCO_2 components in all these applications, and for scales ranging from 5-750 MWe. This work builds upon prior work at SNL, in which sCO_2 component cost models were developed for CSP applications ranging from 1-100 MWe in size.

Similar to the earlier SNL efforts, vendor confidentiality has been maintained throughout this collaboration and in the published results. Cost models for each component were correlated from 4-24 individual quotes from multiple vendors, although the individual cost data points are proprietary and not shown. Cost models are reported for radial and axial turbines, integrally-geared and barrel-style centrifugal compressors, high temperature and low temperature recuperators, dry sCO_2 coolers, and primary heat exchangers for coal and natural gas fuel sources. These models are applicable to sCO_2-specific components used in a variety of sCO_2 cycle configurations, and include incremental cost factors for advanced, high temperature materials for relevant components. Non-sCO_2-specific costs for motors, gearboxes, and generators have been included to allow cycle designers to explore the cost implications of various turbomachinery configurations. Finally, the uncertainty associated with these component cost models is quantified by using AACE International-style class ratings for vendor estimates, combined with component cost correlation statistics.

1 INTRODUCTION

Due to their potential for high efficiency relative to steam Rankine cycles, supercritical CO_2 (sCO_2) power cycles have received increasing attention over the past decade. This assertion is backed by many sCO_2 system studies that maximize the cycle or plant efficiency, although the implications of certain sCO_2 cycle design choices on the plant capital costs are often neglected. For example, selection of low recuperator approach temperatures improve plant efficiency but result in more expensive recuperators due to the increase in surface area required to meet these specifications. Even among sCO_2 systems studies that account for component costs, these costs are highly approximate, and often fail to adequately account for the use of advanced high temperature and pressure alloys that significantly affect component and plant costs.

One of the most significant problems in developing accurate sCO_2 component cost models is the relative infancy of the field relative to conventional technologies. The first operating sCO_2 test loops were only designed and built within the past decade or so, beginning in 2008 with the test loop at SNL [1]. To add to the challenge, the initial test loop sizes have been kW-scale and the designs were generally first-of-a-kind with a sizeable amount of component engineering required. More recently, designs have approached mid-TRL levels and have been scaling up to multi-MW_e sizes that bring more certainty about component costs for commercial-scale systems.

The potential promises of high efficiency, smaller equipment size, and the potential for economic advantage have induced several large and small companies to begin work in sCO_2 system and/or component designs. For example, the number of heat exchanger companies focused on sCO_2 power cycles has increased from one to at least eight in the past ten years. Each of these companies have their own designs and costs that vary across the field.

High fidelity sCO_2 component cost models are required to establish a balance between plant efficiency and cost in the design of a sCO_2 power plant. Such cost models would allow cycle designers to adjust cycle operating conditions to minimize the plant's resulting cost of electricity (COE), which accounts for the cost of the plant's construction annualized over the expected lifetime of the plant. Access to accurate sCO_2 component cost models will enable a paradigm shift in sCO_2 power cycle design studies, away from efficiency-optimized designs and towards COE-minimized designs that include the effects of plant cost in addition to efficiency-derived economic benefits. This shift will accelerate the commercialization of sCO_2 power cycles in general, since penetration into the electric power market is based more on economic competitiveness of the plant as a whole, than on the plant efficiency alone. The present study is focused on meeting this significant need by developing detailed sCO_2 component cost models for a variety of indirect sCO_2 applications, spanning multiple size scales.

1.1 Previous Works

Despite the scarcity of sCO_2 component cost information, several recent studies have attempted to perform the above-suggested COE minimization for sCO_2 plant designs under a variety of applications [2] [3] [4] [5] [6]. However, the component cost models used in these studies were derived from cost models for non-sCO_2 specific equipment, raising uncertainty due to a lack of validation against sCO_2-specific vendor quotes. Other studies have sought to optimize the COE of sCO_2 power plant designs using limited sCO_2 specific equipment cost models and have met with some success [7] [8] [9]. The accuracy and utility of all of the above studies would benefit greatly from sCO_2-specific component cost models.

Studies that have successfully employed sCO_2 component cost models are very few. Studies by NETL on coal-fueled indirect sCO_2 power plants include sCO_2 component costs, though these are generally derived from the literature or from a single vendor's cost information [10] [11]. Plant design studies by Echogen have utilized sCO_2 component cost models that are benchmarked to vendor data, though these models are not publicly available [12] [13]. A techno-economic study of four waste heat recovery cycle configurations was presented using benchmarked heat exchanger cost models but with limited turbomachinery cost models [14]. Another study on sCO_2 recuperators from Zada et al. [15] presented cost ranges benchmarked from 51 estimates from their own design and costing efforts. The most comprehensive sCO_2 component cost modeling effort to date is that of Carlson et al. [16], who scaled non-sCO_2-specific component cost models to fit vendor quotes for sCO_2 components for the purposes of re-evaluating capital costs for a variety of CSP plant designs.

The present study is an extension of this important work in which the component vendor database is expanded, allowing for the development of more sophisticated component cost models. The database presented in this paper is the largest known sCO_2 component cost database, with sources from three DOE National Laboratories, spanning multiple indirect sCO_2 applications and scales. The present work also goes beyond previous efforts by applying a rigorous quality assessment to the quotes, enabling a thorough quantification of uncertainty for the component cost models. These cost uncertainties are an important input in advanced systems modeling platforms that take a rigorous statistical approach to system optimization [17] [18], and to some extent account for the difference between present-day vendor cost estimates and future commercial costs that will be reduced through component refinement and mass production.

2 METHODOLOGY

Commercial competition has forced cost information to remain largely proprietary. This work maintains vendor data confidentiality while leveraging DOE's large database of vendor quotes for sCO_2-specific components. During development of the cost models, the authors withheld vendor identities from one another by redacting all identifying information and sharing only required technical parameters and costs in the database.

In this paper, benchmarked component cost models are presented without disclosing the data or vendors behind the models. For a given component, the resulting cost model is shared, as well as the number of vendor quotes fit with the model, a metric describing the quality of this set of quotes, and the average absolute deviation of these quotes from the model.

Finally, a draft version of this paper was submitted for industry review by companies who maintain their own sCO_2 component cost databases. These reviews qualitatively validate the results of this study, with areas of discrepancy and other feedback from these reviews incorporated in the final paper.

2.1 Sources of Vendor Data

Vendor cost information was sourced from a variety of DOE-contracted scoping studies and vendor surveys from the Offices of Fossil Energy, Nuclear Energy, and Energy Efficiency and Renewable Energy from 2013-2018. Since the cost estimate motivation is unique to each National Laboratory, the collected vendor cost information covers a breadth of scales and designs, enabling a rich and broad dataset.

With the large number of vendor quotes in the database came a wide range of quality. The authors were selective in which quotes to include based on several criteria. The quotes had to be for sCO_2-specific components that can operate at the high pressures and often-high temperatures required. To protect vendor identity and obtain reasonable cost models, all cost models were required to have quotes from at least three different vendors for the specific component, or have at least three vendors that are able to produce such components. Examples of components not included in this work are primary heat exchangers for nuclear and CSP applications, as too few quotes were available. The quotes also had to contain enough technical detail to perform scaling on the relevant parameter, typically shaft power for turbomachinery and conductance-area product for heat exchangers. In some cases, extreme outliers with very high or low costs were excluded. All told, of the 129 vendor quotes collected for this study, 93 were used in the generation of component cost models below.

2.2 Equipment Cost Bases

Where possible, material and labor costs for component installation have been separated from the equipment-only cost, though in some cases, particularly for large-scale systems, installation can constitute a significant fraction of the total cost. Guidance on installation cost estimation for each component can be found in the relevant sections below.

Equipment costs from the various vendor quotes were all baselined to 2017 U.S. dollars using the average Chemical Engineering Plant Cost Index (CEPCI) for 2017, the last full year for which CEPCI values were available for this study. Costs can be translated to another dollar-year basis using the ratio of its CEPCI index to the average 2017 CEPCI index used for this work, 567.5 [19].

Under NETL's standard cost estimating methodology, the equipment cost, combined with the labor and materials installation costs, constitute a Bare Erected Cost (BEC) for a component [20]. To arrive at a Total Plant Cost (TPC), project and process contingencies are added to the BEC for each component/account, as well as fees for the Engineering, Procurement and Construction (EPC) firm to design and build that part of the plant. Contingencies and EPC fees are typically a fixed percentage of the BEC, and typical values are given in Ref [20]. The total cost of a plant is the sum of the TPCs for each of the accounts, and factors heavily into calculating the cost of electricity for the given plant.

As a point of clarification, engineering costs incurred by the EPC firm are typically only for design and integration of the component into the rest of the plant, and are distinct from the engineering costs incurred by a vendor to design and construct their particular component. As sCO_2 power cycles are a new technology, many vendors incur significant non-recurring engineering (NRE) costs to design these new components for construction, which contribute to elevated first-of-a-kind (FOAK) plant costs. Where specified, NRE costs have been subtracted from vendor quotes in this study, which yields a TPC cost basis that is more consistent with existing technologies. Adjustments were not made to quotes to account for unspecified NRE costs.

2.2.1 Turbomachinery Breakdown & Guidance

Depending on the size and application, sCO_2 turbomachinery can be arranged in a variety of ways. Compressors can be on the same shaft as the power turbine or placed on separate shafts with either motor or non-synchronous turbine drives. Power turbines may be coupled to a gearbox for connection to a generator, or above ~65 MWe, can be directly coupled to a synchronous generator and run at 3000 or 3600 rpm, depending on the applicable line frequency [21].

Separate cost correlations have been developed for turbines, compressors, gearboxes, generators and motors, allowing the plant designer to investigate the cost implications of various turbomachinery configurations. For compressor vendor quotes in which motors or turbines were specified as the drivers, these costs have been subtracted from the quotes by using the developed electric motor or turbine cost correlations. Likewise, valve, gearbox and generator costs have been subtracted from supplied turbine vendor quotes to arrive at a turbine-only cost correlation, inclusive of bearing, lube oil, and gas seal equipment required for operation of any turbine.

Useful guidance on appropriate turbomachinery and auxiliary component choices as a function of power was first presented by Fleming et al. [21], and summarized in Figure 1 below. Per their initial turbine scaling estimates, radial turbines are suitable for smaller-scale applications up to ~50 MWe, while axial turbines are more efficient for larger scale applications. Axial turbines are feasible down to sizes of ~7 MWe, though at reduced efficiency relative to radial turbines due to the small size of axial turbine blades at this scale [21]. Based strictly on turbine efficiency, axial turbines are a better choice than radial turbines above ~20 MWe [12], although other considerations may also affect the choice of turbine type, as outlined by Noall [22]. Figure 1 also provides guidance on the use of gearboxes, generators, compressor types, and shaft configurations.

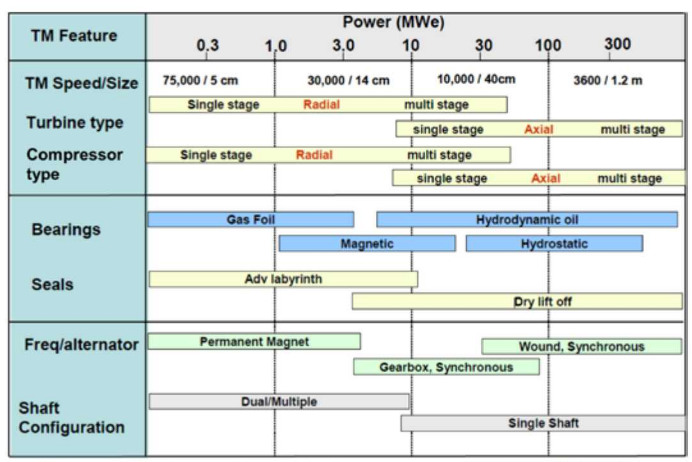

Figure 1. Turbomachinery design type as a function of size, from Fleming et al. [21]

2.2.2 Recuperator Guidance

Closed Brayton cycles rely on a large amount of internal heat recuperation to increase the cycle efficiency. Simple cycles require a single recuperator while recompression sCO_2 Brayton cycle typically have a high temperature recuperator (HTR) and a low temperature recuperator (LTR). Due to high operating pressures of sCO_2 Brayton cycles, compact heat exchangers are typically used because they have lower cost and smaller size than traditional shell and tube heat exchangers. A common design is the Printed Circuit Heat Exchanger (PCHE) that relies on diffusion bonding of plates with chemically-etched microchannels. Other designs include micro-shell and tube as well as plate-fin heat exchangers.

In this work, vendor quotes include all three recuperator design types, and cover a large scale of sizes and temperatures. Heat exchanger costs are closely linked to their thermodynamic size measured by their conductance-area product, UA [16]. The basic equation of $\dot{Q} = UA \times \Delta T_{lm}$ can be used to calculate UA, where $\dot{Q}$ is the thermal duty and ΔT_{lm} is the log mean temperature difference (LMTD), though this equation assumes constant fluid properties within the heat exchanger. For sCO_2, this is a poor assumption in many cases, especially for LTR and sCO_2 cooler conditions. In a typical recompression closed Brayton cycle (RCBC) operating at 550 °C, this causes UA prediction errors of approximately 10% for the HTR and 80% for the LTR. This work considers variable fluid properties by the best practices of using a discretized heat exchanger model with 20 nodes and fluid properties from NIST REFPROP database [23]. In the model, discretization was performed by breaking the total enthalpy change of both fluid streams into equal segments, calculating the segment UAs, and adding these to calculate the total UA. A sensitivity study showed that 20 nodes was sufficient to realize errors less than 1% when compared to 1000 nodes.

2.3 Confidence Ratings

As noted above, there is considerable variability in the quality of the vendor quotes collected for this study. To properly account for these differences, a Confidence Rating (CR) was applied to each quote and used as a weighting factor when deriving component cost correlations.

The Confidence Rating is similar to an AACE International Cost Estimate Classification [24], although it may reflect a reduced quote quality relative to an AACE Classification due to the age of the quote, particularly if advancements have since been made to reduce component costs. The CR, as with the AACE International Cost Estimate Classification, is largely tied to the component design maturity and amount of engineering behind the quote, as summarized in Table 1 [24]. Items included or not included in a quote, as shown at the bottom of Table 1, are rough guidelines used for quote CR assignments in this study.

As a general rule, if quotes did not include adjustments for sCO_2 as a working fluid, they were not considered for inclusion in this study, thus CRs of 1 were not used. A CR of 5 roughly corresponds to as-purchased or off-the-shelf component prices. At the scales considered in this study, very few sCO_2-specific components have been purchased, and none have been included in this study, although CRs of 5 have been used for commercial, non-sCO_2-specific gearboxes and generators in this study.

Table 1: Summary of factors in applying Confidence Ratings to component quotes. Y = Yes, M = Maybe, N = No.

Confidence Rating (CR)	1	2	3	4	5
AACE Class	5	4	3	2	1
Design Maturity	0-2%	1-15%	10-40%	30-70%	65-100%
Uncertainty - Low	-50%	-30%	-20%	-15%	-10%
Uncertainty - High	+100%	+50%	+30%	+20%	+15%
Quote Includes:					
sCO_2-specific	N	Y	Y	Y	Y
Performance estimates	N	M	Y	Y	Y
Cost itemization	N	N	M	Y	Y
Materials of construction	N	N	M	Y	Y
Size and weight	N	N	M	M	Y
Drawings	N	N	N	M	Y
Installation costs	N	N	N	M	Y

2.4 Confidence-Weighted Correlations

Confidence Ratings are used as a “quote multiplier” when developing cost correlations. For example, a quote with a CR of 3 is essentially counted as three identical quotes in the data fit error function that is minimized. A CR-weighted average absolute error between the actual quotes and the component cost model is used, which is defined as:

$$Error = \frac{\sum \left| \frac{Cost_{\text{actual},i} - Cost_{\text{model},i}}{Cost_{\text{actual},i}} \right| CR_i}{\sum CR_i} \quad (1)$$

where CR_i is the Confidence Rating of the i-th quote, and the summations occur over all quotes considered. The coefficients in a given component cost model are adjusted to minimize the Eq. (1) error function. This formulation gives an average uncertainty on the fit of the cost correlation to the data, which is used in the cost model uncertainty quantification below.

Further, an average CR for the collection of vendor quotes used in a particular cost correlation is also reported to give a sense for the level of design and engineering behind these quotes. This is also used to assign high and low uncertainty bounds on the cost correlation, U_{CR}, based on a linear interpolation of Table 1 with the average CR value for the correlation.

2.5 Uncertainty Quantification

There are two independent sources of uncertainty considered in this work: 1) vendor quote confidence rating uncertainty, U_{CR}, discussed above and 2) cost model weighted correlation error (how well the model fits the vendor data). The total cost model prediction uncertainty is propagated from the two sources by the Taylor Series Method of Coleman and Steele [25] as given by:

$$U_{\text{component}} = \sqrt{U_{\text{CR}}^2 + Error^2} \quad (2)$$

where $U_{\text{component}}$ is the total uncertainty in the component cost model and $Error$ is the measure of the model goodness of fit from Eq. (1). This method of uncertainty propagation is the best practice from the field of Verification, Validation, and Uncertainty Quantification. It is also conservative in that the total uncertainty will be greater than either uncertainty alone. Since there are independent low and high uncertainties from the average CR, there will be unique low and high total uncertainties for a given cost model.

3 COMPONENT COST RESULTS

This section includes the basic cost correlation form, correction factor discussions, and the component correlation results and discussion as well as a comparison to previously published results where applicable.

3.1 General Cost Correlation Forms

Following the form of many previous cost models, a power law form is used in this work since it takes advantage of reduced specific costs that are commonly found when scaling to larger sizes. The cost model form is presented below and used throughout this work for consistency:

$$C = a\, SP^b \times f_T \quad (3)$$

where C is the component cost, a and b are fit coefficients, SP is the scaling parameter, and f_T is a temperature correction factor described in the following section. This form has the advantage of adapting to nonlinear and linear cost trends.

3.2 Correction Factor Considerations

3.2.1 Temperature Correction Factor

Supercritical CO_2 component costs can vary considerably with service temperature due to upgrades in the required materials of construction for sCO_2 power cycles. A recent component cost modeling effort by Mecheri [26] included cost correction factors to account for material selection and thickness as a function of temperature and pressure. Where appropriate, temperature corrections were applied following the form:

$$f_T = \begin{cases} 1 & if\ T_{max} < T_{bp} \\ 1 + c\left(T_{max} - T_{bp}\right) + d\left(T_{max} - T_{bp}\right)^2 & if\ T_{max} \geq T_{bp} \end{cases} \quad (4)$$

where T_{bp} is the temperature breakpoint, typically 550 °C, and T_{max} is the maximum temperature rating of the component, in units of °C. Based on conventional experience, the temperature breakpoint of 550 °C roughly corresponds to the temperature at which thinner, more expensive tube materials such as nickel-based superalloys become more cost-effective than thicker, low-cost stainless steels.

3.2.2 Pressure Correction Factor

Overall, vendor quotes compiled in this study were for sCO_2 power cycles within a narrow range of operating pressures around 250-300 bar. Pressure correction factors were investigated in cost models for recuperators and primary heaters, but were not used as no obvious trend was observed and the narrow range provides little basis for differentiation. Intuitively, costs will increase with pressure, but cycle efficiency will increase as well. Future work could develop a correction factor to enable economic optimization with pressure.

3.2.3 Pressure Drop Correction Factor

For recuperators and primary heaters, the influence of pressure drop on cost was investigated but the data were not sufficient to develop a suitable correlation. This is likely due to relatively large cost variabilities between vendors, introducing noise that overwhelms inherent trends that should exist. Future work could include a comprehensive study of pressure drop's influence on cost from a single vendor, such as an extension on the cost modeling work of Zada et al. based on 51 quotes from a single vendor [15].

3.3 Primary Heaters

Primary heaters vary significantly in structure and cost, depending on the indirect sCO_2 application. Of the various applications, a sufficient number of vendor quotes for generation of component correlations were only available for natural gas- and coal-fired primary heaters. Primary heater costs for nuclear, concentrated solar, and waste heat recovery applications are not included in the present study, but may be developed in future work.

Being combustion-driven applications, the physical implementation of natural gas- and coal-fired primary heaters is expected to be similar, namely in that sCO_2 is heated both radiantly and convectively in a series of tube banks, similar to those used in a steam boiler. Since boiler tube selection does not vary appreciably with the choice of fuel or thermal duty of the boiler, it was assumed that boiler tube material selection would be driven only by boiler code temperature and pressure limitations. As a result, a single temperature correction factor was derived for use with both coal- and natural gas-fueled primary heaters:

$$f_{T,PHX} = \begin{cases} 1 & if\ T_{max} < 550\ °C \\ 1 + 5.4 \times 10^{-5}(T_{max} - 550\ °C)^2 & if\ T_{max} \geq 550\ °C \end{cases} \quad (5)$$

For heat exchanger equipment, costs typically scale with UA. However, this is difficult to calculate *a priori* without knowledge of the fuel combustion characteristics, primary heater layout, and breakdown of convective vs. radiant heat transfer modes. As a result, cost correlations based on thermal duty scaling are provided.

3.3.1 Coal-fired

Cost correlation of pulverized coal-fired (PC) sCO_2 primary heaters is assumed to be of form,

$$C_{CF,PHX} = a\, Q^b \times f_{T,PHX} \quad (6)$$

where, $C_{CF,PHX}$ is the cost of coal-fired primary heater in 2017\$, Q is the thermal heat duty in MW_{th} and $f_{T,PHX}$ is the temperature correction factor described in Eq. (5). The coefficients a and b are calculated by minimizing the confidence-weighted average absolute error (from Eq. (1)) of four primary heater cost estimates from an EPRI study [13], with an average Confidence Rating of 4.0 and thermal heat duty from 187 – 1,450 MW_{th}.

$$C_{CF,PHX} = 820{,}800\ Q^{0.7327} \times f_{T,PHX} \quad (7)$$

The correlation described in Eq. (7) yields a CR-weighted average absolute error of ±17%. This error, combined with the uncertainty due to the average CR of the quotes, gives an overall uncertainty of -23% to +26% for this correlation using Eq. (2). While this uncertainty is fairly low, it is very restrictive in that it is derived from one vendor's estimates for a particular inverted downdraft heater design, with the attendant flue gas to tube bank temperature differences. The correlation in Eq. (7) is inclusive of burners, fans, air preheaters, ductwork, headers, and interconnecting piping, and is valid for sCO_2 temperatures up to 730 °C and pressures of 260-310 bar.

As mentioned above, heat exchanger costs typically scale better with UA rather than heat duty. If desired, the following alternative scaling can be used for cost estimation of coal-fired primary heaters of the type in EPRI's study, with valid UA values ranging from $7.4\text{x}10^5$ to $5.9\text{x}10^6$ W/K:

$$C_{CF,PHX} = 1{,}248\ UA^{0.8071} \times f_{T,PHX} \quad (8)$$

In using Eq. (8), the coefficient $5.4\text{x}10^{-5}$ in Eq. (5) for $f_{T,PHX}$ should be replaced with $5.3\text{x}10^{-6}$. The correlation described above yields a CR-weighted average absolute error of ±2.7%. This error, combined with the uncertainty due to the average CR of the quotes, gives an overall uncertainty of -16% to +21%, with similar caveats as those attached to the use of Eq. (7).

Materials and direct labor costs needed for installation of the primary heater should be added to the equipment cost to determine a BEC or "as-built" cost for the primary heater. In general, coal-fired heaters are built on-site, thus the installation materials cost is usually included in the equipment cost. Labor costs for installation can vary widely and will depend on prevailing wage rates at the plant location. Primary heater installation labor costs from the ERPI study were assessed [13], as well as comparable steam boiler costs from Ref. [27]. Based on these studies, an installation labor cost of 50% of the equipment cost is recommended as a rough guideline for estimation purposes.

3.3.2 Natural Gas-fired

The cost correlation for natural gas-fired primary heaters is based on 10 vendor cost estimates in the 10-50 MW_{th} range, with an average CR of 3.0 across the data set. The vendor estimates include burners, emissions controls, and air preheaters, and cover heaters both with and without radiant sections. For this range, the cost correlation, of the form of Eq. (6), is:

$$C_{NG,PHX} = 632{,}900\ Q^{0.60} \times f_{T,PHX} \quad (9)$$

The power law exponent on the thermal duty for this correlation is based on the power law scaling of a set of quotes from a single vendor spanning the thermal duty range, since the remaining quotes are tightly grouped in the 20-30 MW_{th} range and are poorly-suited for deriving an appropriate power law exponent. The power law exponent of 0.60 is similar to that in conventional steam boilers, where exponents ranging from 0.581 to 0.694 are used [28] [29].

Based on the vendor quotes, this correlation yields a CR-weighted average absolute error of ±15%. Combined with the uncertainty of the quotes through the average CR, the uncertainty of this correlation is estimated as -25% to +33%. As with the coal-fueled PHX correlation, a more robust UA-based scaling could likely be achieved if such data were available in the quotes. Equation (9) is valid for sCO_2 pressures from 230-275 bar, and temperatures up to 715 °C.

At the smaller scales for which this cost correlation is applicable, natural gas-fueled primary heaters (or sections of them) may be manufactured offsite and delivered to the plant location for installation. Based on the vendor quotes received, as well as Heat Recovery Steam Generators for natural gas combined cycle plants [27], which serve similar functions to their sCO_2 primary heater counterparts, installation costs of 8% for materials, and 12% for labor, relative to equipment costs, are recommended.

3.4 Recuperators

A total of 24 vendor quotes were used to develop the recuperator model, including both HTRs and LTRs. These recuperator vendor quotes had a UA range of 1.60 $\text{x}10^5$ to $2.15\text{x}10^8$ W/K and thermal duty range of 5 to 3000 MW_{th}. The maximum hot circuit temperatures ranged from 407-584 °C for HTRs and 165-252 °C for LTRs. The maximum pressures on the cold circuit were 210-320 bar with deviations of less than 10 bar between HTRs and LTRs. The pressure drops ranged from 0.70-4.0 bar with a negligible deviation of 0.005 bar.

In analyzing the data, individual cost models were considered for HTRs and LTRs, but better scale coverage was obtained by combining both recuperator types. A recent study analyzed cost estimates from 51 heat exchangers and suggested that LTRs should have a 20% lower cost than HTRs [15]. The current work includes temperature scaling that is designed to account for these cost differences in a similar manner. Consideration was also given to PCHE and non-PCHE groupings, but again there was little difference in resulting models so a combined approach was used.

The recuperator cost model follows the same form as for primary heaters and is shown below.

$$C_{\text{Recup}} = 49.45\ UA^{0.7544} \times f_{T,\text{Recup}} \quad (10)$$

$$f_{T,\text{Recup}} = \begin{cases} 1 \ if\ T_{max} < 550\ °\text{C} \\ 1 + 0.02141(T_{max} - 550\ °\text{C})\ if\ T_{max} \geq 550\ °\text{C} \end{cases} \quad (11)$$

The temperature breakpoint T_{bp} in Eq. 10 was chosen to be 550°C due to the trend of the ASME Boiler and Pressure Vessel Code (BPVC) allowable stress curve for 316 stainless steel (SS), which is often used in the design of recuperators up to 550-600 °C. The allowable stress is constant up to 150 °C, decreases slightly between 150 °C and 550 °C, and drops drastically above 550 °C. Of the twenty-four quotes, four were at temperatures above 550 °C. Of these, two have confirmed use of 316 SS up to 580 °C and two did not specify the material. The temperature correction factor, $f_{T,\text{Recup}}$, was best fit with only the linear coefficient c from Eq.(4). The value of c near 0.02 has the effect of approximately doubling the cost at 600 °C, tripling at 650 °C.

The average CR for the quotes in the recuperator cost scaling is 3.125. Using linear interpolation to uncertainties in Table 1, the resulting low and high uncertainties are -19% and +29%, respectively. The weighted average error of the correlation is ±24%. Therefore, the total uncertainties of the recuperator model are -31% and +38%.

The current cost model can be compared with those published by Carlson et al. [16] and Zada et al. [15] that are recent works, sCO_2-specific, and benchmarked with vendor quotes. The Carlson work presented cost models in the form of $C = a\, C^*\, UA$ where C^* is an extra scaling factor for UA values smaller than 10^6 W/K where costs may reflect a sizeable amount of engineering. It had a range of C^* of 1.0 for $UA = 10^6$ W/K that increased nonlinearly to 6.3 as UA decreased to $5\text{x}10^3$ W/K. The Zada work had a simpler form of $C = a\, UA$. Both of these linear forms were considered in this work but did not fit the data well, as the specific cost ($/(W/K)) decreased noticeably with increasing UA. The Carlson value of a was a range of 1.1-4.0 $/(W/K) for his vendor quote baselined recommendation [16]. For the Zada work, the value of a was 1.49-2.21 $/(W/K) for HTRs and 1.19-1.77 $/(W/K) for LTRs, noting that the values for LTRs are 20% lower [15]. This lower cost is due to lower design temperatures and the subsequent higher allowable stress enabling less material use.

For comparison of the current model to those published previously, the averages in the ranges were used. The results are shown in Figure 2, where the temperature factor for the current model was 1.0, relating to the average HTR hot inlet temperature of 488 °C in the vendor quotes. It is very consistent with the Carlson model at the low range, with the Zada models near UA=10^6 W/K, but predicts lower cost for larger values of UA. The deviations between the current model and the published models are shown on the second y axis. There are deviations that are outside of the current model's uncertainties for both small and large scales. For larger scales above 10^6 W/K, the specific costs are trending down with size. Industry feedback on these results suggested that the current model is most accurate at large scales, including a desirable power law coefficient that is consistent with their observations. Industry feedback also suggested the Zada model is more accurate for $UA < 10^6$ W/K. Note that the Carlson line is solid in the area of benchmarking and dotted where it is extrapolated. The Zada paper was benchmarked for a much larger range of UA and is therefore not extrapolated in this view.

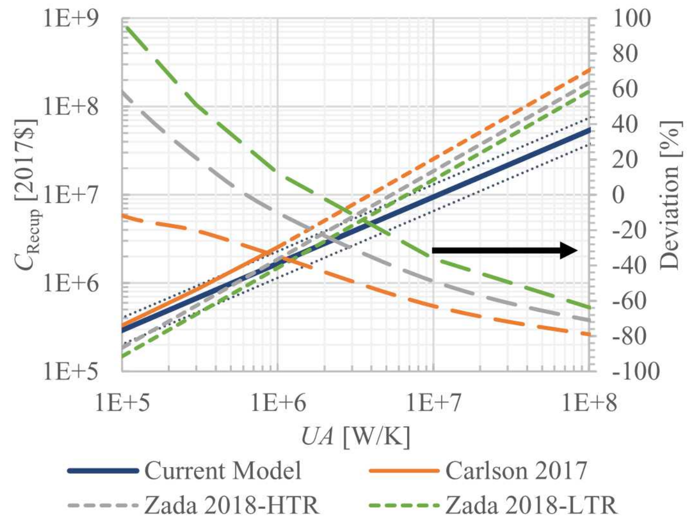

Figure 2. Recuperator model cost trend compared with published models [15] [16]. Dotted lines above and below the current model indicate the uncertainty bounds of +38% to -31%, respectively.

As modular, stationary components, recuperator installation costs reported in several studies are relatively low. Recommended installation costs relative to equipment costs are 2% for materials and 3% for labor.

3.5 Direct Air Coolers

The cooling units in this study are direct dry air coolers with crossflow configuration. They have sCO_2 flowing inside finned-tube banks and fans blowing air outside, similar to those proposed in several recent sCO_2 plant design studies [7] [8] [9]. An alternative cooling strategy is to cool the sCO_2 with water from a cooling tower or other process, in which case a PCHE or microtube heat exchanger could be used for the water/sCO_2 cooler. For this approach, the water/sCO_2 heat exchanger cost would be similar to recuperators, though a specific cost model was not developed for this study. Using the recuperator model is likely conservative since they require high pressure on both circuits and the water/sCO2 has low pressure on one side, reducing thickness requirements. The water to air cooling unit could then be estimated from industrial units that are expected to be 'off-the-shelf'.

The cost correlation for the direct dry sCO_2 air coolers is assumed to be of the form,

$$C_{\text{dry cooler}} = a\, UA^b \tag{12}$$

where $C_{dry,cooler}$ is the cost of direct dry air cooler in 2017$ and UA is the overall conductance in W/K. As temperatures are low, no temperature correction factor is required. It should be noted that estimation of UA for sCO_2 direct dry air coolers is not straightforward primarily due to two factors. Firstly, the sCO_2 coolers operate close to the critical point where the thermophysical properties of CO_2 vary drastically through the cooler. Secondly, the fluid flow arrangement in direct dry coolers is often complex including multiple tube rows and passes. Therefore, a discretized approach needs to be adopted for an accurate estimation of the overall conductance as noted by Pidaparti et al. [8] among others. The authors recommend Ref [30] for a description of a detailed mathematical model for the calculation of *UA* for cross-flow heat exchangers using a discretized approach. This method is used for calculation of *UA* when no values are provided in the vendor quotes.

Eq. (13) presents the coefficients *a* and *b* from Eq. (12), obtained by minimizing the confidence-weighted average absolute error of 11 quotes from 7 different vendors with an average CR of 4.0 and UA ranging from 8.6x10^5 to 7.5x10^7 W/K.

$$C_{\text{dry cooler}} = 32.88\, UA^{0.75} \tag{13}$$

The maximum CO_2 temperatures ranged from 50-170 °C for ambient temperatures ranging from 5-35 °C. The maximum pressures of CO_2 were 54-100 bar and pressure drops ranged from 0.5-1.5 bar. The direct dry sCO_2 air cooler cost correlation described in Eq. (13) predicted the vendor prices with a confidence-weighted average absolute error of ±20%. Combined with the uncertainty in the vendor quotes through average CR, the estimated uncertainty for the cost correlation is -25% to +28%.

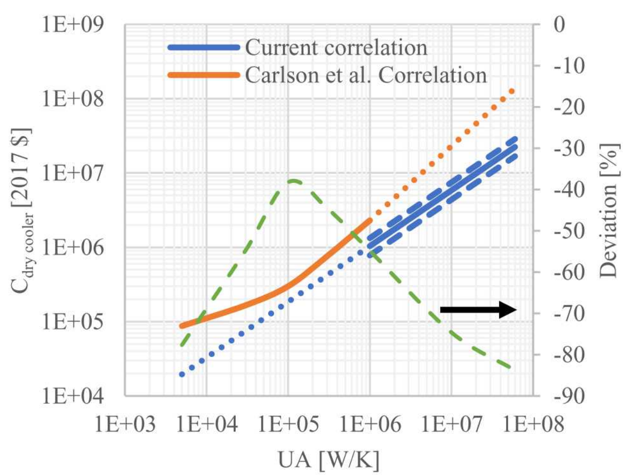

Figure 3. Comparison of direct dry sCO_2 air cooler cost correlation with that from Carlson et al. [16] Dotted lines above and below the current correlation indicate the uncertainty bounds of +28% and -25%, respectively.

Figure 3 compares the cost correlation proposed in Eq. (13) with the correlation proposed by Carlson et al. [16]. The dashed line for the Carlson et al. and current correlation in Figure 3 indicates that the correlations have been extrapolated out of the range of their validity. At large values of $UA > 10^6$ W/K, the Carlson correlation is shown to over-predict the direct dry sCO_2 air cooler costs given by Eq. (13), since it was baselined for low values of $UA < 10^6$ W/K using sCO_2 specific vendor quotes as well as non-sCO_2 specific data from literature. Only sCO_2-specific data was included in the present study, however, based on the differences in the trends between two correlations in Figure 3, it is possible that the correlation of Eq. (13) will change slightly if vendor quotes with $UA < 10^{-6}$ W/K are included.

Based on EPRI's study [13], as well as NETL's internal plant cost studies on dry cooling technologies, recommended installation costs relative to equipment costs are 8% for materials and 12% for direct labor.

3.6 Turbomachinery

As noted in Section 2.2.1, turbomachinery costs have been broken down into individual components to allow for economic evaluation of various turbomachinery arrangements, such as turbine-driven vs. motor-driven compressors, systems with the turbine, compressors and generator on a single shaft, etc. Turbines have been further subdivided into radial and axial turbines, while compressors have been subdivided into integrally-geared and barrel-type centrifugal compressors below.

3.6.1 Turbines

The developed cost scaling model for both axial and radial turbines uses the turbine shaft power, $\dot{W}_{sh}$, as the primary scaling parameter, in units of MW_{sh}:

$$C = a\, \dot{W}_{sh}^{b} \times f_T \tag{14}$$

Note from Section 2.2.1 that this model is intended to reflect turbine-only cost scaling, and is exclusive of turbine stop & control valves, gearbox (if needed), and generator, though it does include bearings, seals, and associated equipment.

The cost correlation for radial turbines is based on a small set of four vendor estimates, with an average CR of 2.0, and a range of 8-35 MW_{sh}. The resulting cost model is:

$$C_{t,\text{rad}} = 406{,}200\, \dot{W}_{sh}^{0.8} \times f_{T,\text{rad}} \tag{15}$$

$$f_{T,\text{rad}} = \begin{cases} 1 & if\ T_{max} < 550\ °C \\ 1 + 1.137\text{x}10^{-5}(T_{max} - 550\ °C)^2 & if\ T_{max} \geq 550\ °C \end{cases} \tag{16}$$

Equation (15) is valid for single stage radial turbines with temperatures up to 700 °C and inlet pressures from 200-260 bar. In this correlation, the power law exponent was limited to a value of 0.8, though the best fit value was larger than this due to subtraction of gearbox and generator costs. The resulting CR-weighted average absolute error was ±11.9%, though this is due to the large number of fitting parameters relative to the number of vendor quotes in the fit. Given that the quotes are based on a relatively low level of engineering, the correlation uncertainty of -32% to +51% is dominated by the CR of the quotes. Due to this high uncertainty, the Eq. (15) cost scaling relationship is a target for improvement in future studies.

The axial turbine cost model is based on six vendor quotes with a higher average CR of 3.7 and spanning a shaft power range of 10 – 750 MW_{sh}. Following the cost scaling model of Eq. (14) above, the best-fit correlation is:

$$C_{t,ax} = 182{,}600\, \dot{W}_{sh}^{0.5561} \times f_{T,ax} \quad (17)$$

$$f_{T,ax} = \begin{cases} 1 & if\ T_{max} < 550\ ℃ \\ 1 + 1.106 \times 10^{-4}(T_{max} - 550\ ℃)^2 & if\ T_{max} \geq 550\ ℃ \end{cases} \quad (18)$$

For this correlation, the average absolute error is ±19%. Combined with the uncertainty in the vendor quotes, the cost correlation uncertainty is estimated as -25% to +30%. Equation (17) is valid for turbine inlet temperatures up to 730 °C, and for inlet pressures of 240-280 bar.

The axial turbine-only cost correlation from Eq. (17) is compared to EPRI's cost models [13] at turbine inlet temperatures of 593 °C and 730 °C, in Figure 4. The EPRI correlation, which is based on three turbine quotes, appears to fall within the correlation uncertainty bounds for high temperature turbine cases but may overpredict turbine costs for the lower-temperature turbines.

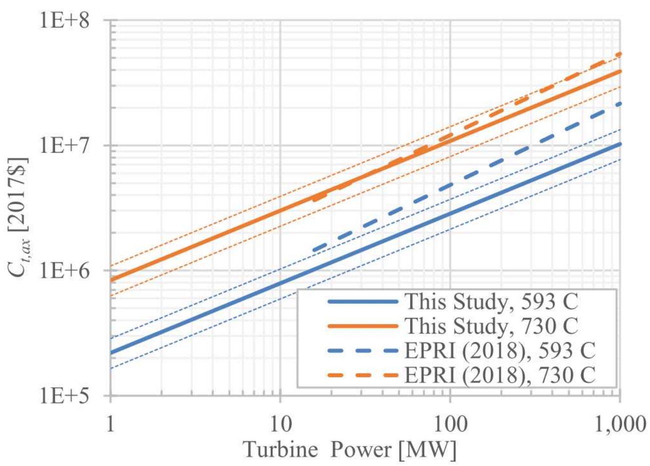

Figure 4. Axial turbine cost scaling models from this study, compared to that of EPRI [13]. Dotted lines above and below this study's results correspond to uncertainty bounds of +30% and -25%, respectively.

Based on sCO_2-specific studies, as well as steam turbine installation factors [27], the recommended installation costs for radial and axial turbines are 8% for materials, and 12% for direct labor, relative to equipment costs.

3.6.2 Compressors

As described earlier, sCO_2 compressors are grouped into integrally geared (IG) centrifugal and barrel-type centrifugal compressor categories. Cost correlations were developed for each of these compressor types separately. Cost correlation of IG centrifugal compressors is assumed to be of form,

$$C_{IG} = a\, \dot{W}_{\text{sh}}^{\ b} \quad (19)$$

where, C_{IG} is the cost of IG centrifugal compressors and $\dot{W}_{sh}$ is the compressor shaft power in MW_{sh}. The coefficients a and b are calculated by minimizing the confidence weighted average absolute error of 15 IG centrifugal compressors from three vendors with an average confidence rating of 2.67 and $\dot{W}_{sh}$ ranging from 1.5 to 200 MW_{sh}. The resulting cost correlation is:

$$C_{IG} = 1{,}230{,}000\, \dot{W}_{\text{sh}}^{\ 0.3992} \quad (20)$$

The IG centrifugal compressors cost correlation described in Eq. (20) predicted the vendor prices with a confidence-weighted mean average error of ±31.5%. Combined with the uncertainty in the vendor quotes, the cost correlation uncertainty is estimated as -39% to +48%. Equation (20) is valid for compressor inlet and outlet pressures ranging from 65-90 bar and 245-345 bar respectively.

Figure 5 compares the cost correlation proposed in Eq. (20)with the correlation proposed by Carlson et al. [16] that has been baselined to vendor quotes with $\dot{W}_{sh}$ ranging from 1.5 – 25 MW_{sh}. The dotted line in Figure 5 indicates that the Carlson correlation has been extrapolated out of the range of its validity. The current correlation predicts much lower IG centrifugal compressor costs at higher power levels, and the reasons for differences between these correlations are unclear. However, industry feedback indicated that Eq. (20) is more accurate than the Carlson correlation in predicting IG compressor costs, but underpredicts the costs for high-end engineered IG compressors with power levels < 1 MW_{sh}.

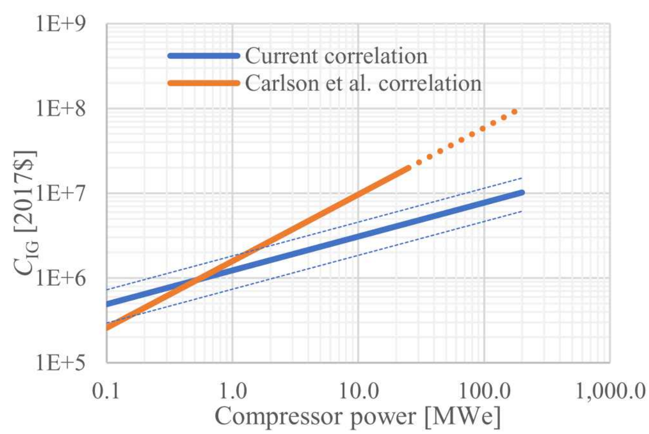

Figure 5. Comparison of IG centrifugal cost correlation with existing correlations from open literature. Dotted lines above and below the current correlation indicate the uncertainty bounds of +48% and -39%, respectively.

The cost correlation for barrel-type centrifugal compressors is assumed to be of the form of Eq. (21) since the cost of barrel-type machines typically scales better with volumetric flow.

$$C_{\text{barrel}} = a\, \dot{V}_{in}^{\ b} \quad (21)$$

In Eq. (21), C_{barrel} is the cost of barrel-type centrifugal compressors and $\dot{V}_{in}$ is the volumetric flow rate at inlet in m^3/s.

The coefficients a and b are calculated by minimizing the confidence weighted average absolute error of four barrel-type centrifugal compressor quotes from one vendor with an average confidence rating of 2.0 and $\dot{V}_{in}$ ranging from 0.1 – 2.4 m^3/s. The resulting cost correlation is:

$$C_{\text{barrel}} = 6{,}202{,}000\,\dot{V}_{in}^{\;0.1114} \qquad (22)$$

The barrel-type centrifugal compressor cost correlation described in Eq. (22) predicted the vendor prices with a confidence-weighted mean average error of ±4.6%. Combined with the uncertainty in the vendor quotes, the estimated uncertainty of the cost correlation is -30% to +50%. Equation (22) is valid for compressor inlet and outlet pressures ranging from 76-82 bar and 210-250 bar respectively.

As pointed out in Sec 2.2.1, the compressor cost correlations described in this section exclude the driver costs. This allows the plant designer to select either motor or turbine drive for the compressors depending on the design requirements and also to explore cost trade-offs between different driver options. Owing to the high uncertainties associated with sCO_2 compressor cost correlations, it is recommended that these correlations be revisited when more vendor quotes with higher confidence rating are available from multiple vendors in the future.

Similar to turbines, recommended compressor installation costs are 8% for materials, and 12% for direct labor, relative to equipment costs.

3.6.3 Valves

A number of vendor estimates were collected for turbine stop and control valves, however, a reasonable cost scaling equation could not be derived for these components. The appropriate choice of scaling parameter is not obvious for these components, as suitable scaling could not be obtained as a function of mass flow, volumetric flow, or valve body diameter. Valve costs are also significantly affected by required response times and allowable pressure drops. Further, due to the wide variety of materials and service temperatures included in these quotes, a temperature correction factor is recommended for this cost correlation. In short, the available quotes did not have enough consistent design parameters between them to enable the development of a cost correlation on a common basis. Additional quotes and clarity on appropriate scaling parameters will be pursued in future work.

3.6.4 Gearboxes

Gearboxes are required for reducing the high turbine shaft speeds that are required for high turbine efficiency at small sizes to a synchronous generator shaft speed. In general, vendor quotes reveal that gearboxes for generator speeds of 3600 RPM are almost half the cost of gearboxes for 1800 RPM generators, due to the difference in gear ratio. However, the very high cost of 3600 RPM generators relative to their 1800 RPM counterparts generally results in an 1800 RPM gearbox and generator as being the most economic combination of components for power generation.

The cost correlation below is derived from seven vendor quotes for epicyclic and parallel-shaft gearboxes with 1800 RPM generator shaft connections, with an average vendor quote CR of 4.1. The cost correlation uses the turbine shaft power, $\dot{W}_{sh}$, as the primary scaling parameter, in units of MW$_{\text{sh}}$:

$$C_{\text{Gearbox}} = 177{,}200\,\dot{W}_{sh}^{0.2434} \qquad (23)$$

This correlation only covers a small range of gearbox sizes from 4 to 10 MW$_{\text{sh}}$ with turbine shaft speeds from 25,000-29,000 RPM, thus it is a likely candidate for improvement to cover larger sizes and 3600 RPM synchronous speeds in future studies. The CR-weighted absolute error between the correlation and vendor quotes is ±5%, which yields a correlation uncertainty of -15% to +20% when combined with the vendor quote uncertainty.

Installation factors for gearboxes are taken to be the same as for turbines, 8% for materials and 12% for direct labor, relative to equipment costs.

3.6.5 Generators

The generator cost correlation is derived from eight vendor quotes with an average CR of 4.0. The correlation scales with electric power output, $\dot{W}_e$ in units of MW$_e$ and covers scales from 4 to 750 MW$_e$. Generators included at small scales (< 65 MW$_e$) are 4-pole, 1800 RPM generators, transitioning to 2-pole, 3600 RPM generators at larger scales:

$$C_{\text{Generator}} = 108{,}900\,\dot{W}_e^{0.5463} \qquad (24)$$

The weighted average absolute error for this correlation is ±12%. Including the uncertainty in the vendor quotes, the estimated uncertainty for this cost correlation is -19% to +23%.

Installation factors for generators are taken to be the same as for turbines, 8% for materials and 12% for direct labor, relative to equipment costs.

3.6.6 Motors

Cost correlations of various compressor motor drives are derived from Aspen Process Economic Analyzer [31]. Described below are the cost correlations for three different motor drive offerings and their range of validity. Figure 6 exhibits the cost correlation trends of these three different motor offerings. Depending on the power level, the most economic motor can be selected from these offerings. Since the motor cost correlations are derived from a software package and the motors are components with high TRL, a CR of 4.0 is assigned to the motor costs. This implies that the expected uncertainty of the motor cost correlations is -15% to +20%.

Explosion proof motors ($0.00075 \le \dot{W}_e \le 2.8$) MW$_e$:

$$C_{\text{EPM}} = 131{,}400\,\dot{W}_e^{\;0.5611} \qquad (25)$$

Synchronous motors ($0.15 \le \dot{W}_e \le 15$) MW_e:

$$C_{SM} = 211{,}400\ \dot{W}_e^{\ 0.6227} \tag{26}$$

Open drip-proof motors ($0.00075 \le \dot{W}_e \le 37$) MW_e:

$$C_{OM} = 399{,}400\ \dot{W}_e^{\ 0.6062} \tag{27}$$

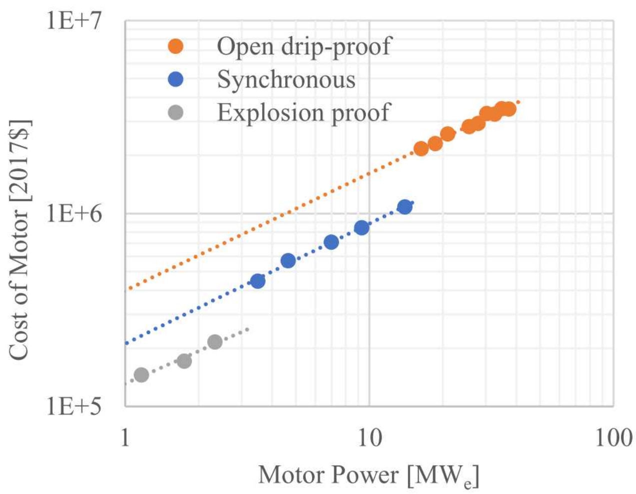

Figure 6. Comparison of cost of different motor offerings from Aspen Process Economic Analyzer [31]

Similar to other turbomachinery, motor installation costs are recommended as 8% for materials and 12% for labor, relative to equipment only costs.

3.6.7 Turbomachinery Cost Model Comparison

For purposes of comparison, the cost models in Eq. (17), (23), and (24) for axial turbines, gearboxes, and generators, respectively, are combined and compared to results from other studies in Figure 7. In particular, costs are compared to Carlson's sCO_2-specific turbine costs at turbine inlet temperatures of 700 °C [16], and to non-sCO_2-specific turbogenerator costs used by Wang for sCO_2 turbine sets [4]. Note that the present cost model yields a slight reduction in cost above 65 MW, where the axial turbine can be designed to operate at synchronous speeds and a gearbox is no longer needed. Results show that Carlson's turbogenerator set costs are generally overpredicted relative to the correlations derived in this study, with increasing deviation as turbine shaft power increases due to the emergence of reliable turbine quotes in this high power range. The cost correlation employed by Wang, derived for non-sCO_2 turbomachinery, uses a power law exponent of 0.81, which yields significant differences from the sCO_2-specific correlation derived in this study for high and low turbine shaft power [4].

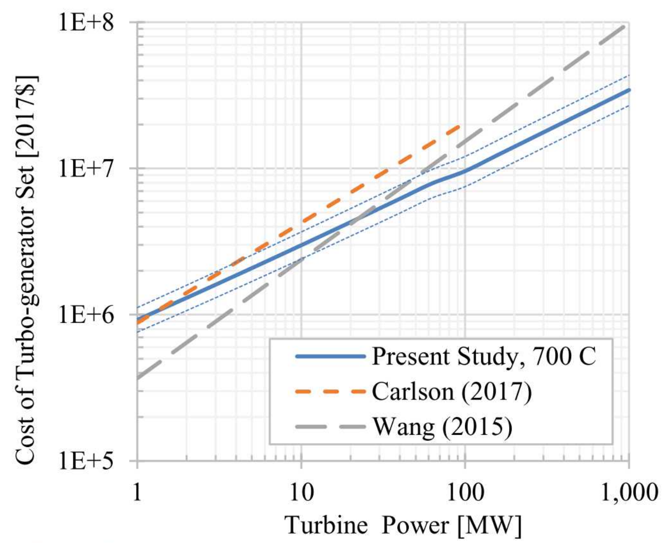

Figure 7. Comparison of turbo-generator set costs at turbine inlet temperatures of 700 °C, in comparison to correlations from Carlson et al. [16], and Wang et al. [4]. The present study costs include an axial turbine, a generator, and for turbine power below 65 MW, a gearbox, with combined uncertainty shown by the dotted lines.

3.7 Other Components

It should be noted that the above sCO_2 component cost correlations cover most, but not all, of the costs for the sCO_2 power block in a plant. The most significant omission is the cost of the sCO_2 piping, which may constitute 5-20% of the cost of the sCO_2 power block [10]. These costs can be calculated following the approach of Walker et al. [32]. If nickel alloy piping is required for high temperature cycle operation, costs are in the upper portion of this range, and cycles with reheat incur additional costs for the extra piping runs between the primary heater and reheat turbine [10].

Another component that was intentionally omitted is the inventory control system. As it is a mature technology and sCO_2-specific, it is expected to be 'off-the-shelf'.

Finally, many other costs must be added to the sCO_2 power block cost to determine the bare erected cost of the plant, including those for fuel and waste handling, electrical accessories, instrumentation and controls, site preparation, and buildings and foundations. Further, engineering, indirect (administrative) labor, and project and process contingencies are added to yield a total plant cost. Procedures for estimating these costs can be found in NETL's Quality Guidelines for Energy Systems Studies [20] [28].

3.8 Summary of Cost Correlations

This section summarizes the cost correlations described in the previous sections. The cost correlations of all the components assume a generalized correlation of form Eq. (3). Table 2 summarizes the scaling parameters (*SP*) used for deriving the cost correlations of all the components and the corresponding curve fitting coefficients $a, b,\ c$, and d. Coefficients c and d account for the temperature correction factor from Eq. (4). Where applicable, a temperature breakpoint of 550 °C was used in the temperature correction factor. Also summarized in Table 2 are the range of validity and uncertainty ranges for all the component cost correlations. Out of all the components from Table 2, the radial turbines and the compressors exhibit large uncertainties due to the lack of high-quality vendor quotes in this study. These cost correlations will be revisited in the future as the technology matures and more high-quality vendor quotes become available.

Table 2. Summary of the scaling parameters and coefficients for all the components considered in the current study along with their range of validity and uncertainty ranges.

Component	Scaling parameter (Units)	Coefficients from Eq. (3) and Eq. (4)				Database range (Range of validity)	Uncertainty range
		a	b	c	d		
Coal-fired heaters	Q (MW_{th})	820,800	0.7327	0	5.4e-5	187 to 1,450 MW_{th}	-23% to +26%
Natural gas-fired heaters	Q (MW_{th})	632,900	0.60	0	5.4e-5	10 to 50 MW_{th}	-25% to +33%
Recuperators	UA (W/K)	49.45	0.7544	0.02141	0	1.6e5 to 2.15e8 W/K	-31% to +38%
Direct air coolers	UA (W/K)	32.88	0.75	0	0	8.6e5 to 7.5e7 W/K	-25% to +28%
Radial turbines	$\dot{W}_{sh}$ (MW_{sh})	406,200	0.8	0	1.137e-5	8 to 35 MW_{sh}	-32% to +51%
Axial turbines	$\dot{W}_{sh}$ (MW_{sh})	182,600	0.5561	0	1.106e-4	10 to 750 MW_{sh}	-25% to +30%
IG centrifugal compressors	$\dot{W}_{sh}$ (MW_{sh})	1,230,000	0.3992	0	0	1.5 to 200 MW_{sh}	-40% to +48%
Barrel type compressors	$\dot{V}_{in}$ (m^3/s)	6,220,000	0.1114	0	0	0.1 to 2.4 m^3/s	-30% to +50%
Gearboxes	$\dot{W}_{sh}$ (MW_{sh})	177,200	0.2434	0	0	4 to 10 MW_{sh}	-15% to +20%
Generators	$\dot{W}_{e}$ (MW_{e})	108,900	0.5463	0	0	4 to 750 MW_{e}	-19% to +23%
Explosion proof motors	$\dot{W}_{e}$ (MW_{e})	131,400	0.5611	0	0	0.00075 to 2.8 MW_{e}	-15% to +20%
Synchronous motors	$\dot{W}_{e}$ (MW_{e})	211,400	0.6227	0	0	0.15 to 15 MW_{e}	-15% to +20%
Open drip-proof motors	$\dot{W}_{e}$ (MW_{e})	399,400	0.6062	0	0	0.00075 to 37 MW_{e}	-15% to +20%

4 EXAMPLE OF PLANT COST ESTIMATION

The cost models described in this paper can be used to estimate the total equipment cost of the sCO_2 power block for a wide range of applications with reasonable accuracy. Table 3 presents example calculations of sCO_2 power block equipment costs for a 10 MW_e plant similar to the STEP facility, and a large scale 550 MW_e utility plant, based on the Baseline620 case from a previous NETL study [10]. The operating conditions for the 10 MW_e plant are taken from Zitney and Liese [33], and correspond to the simplified block flow diagram and steady state operating conditions shown in Annex A. The block flow diagram and operating conditions for the NETL Baseline620 case can be found in Ref [10]. The turbine inlet temperature for the 10 MW_e plant is 700 °C and for the NETL Baseline620 case is 620 °C.

For the 10 MW_e plant, both compressors are assumed to be integrally-geared centrifugal machines driven using explosion-proof motors since they are more economical at small scales. For the NETL Baseline620 case, the main compressor and recompressor are assumed to be barrel-type machines driven with open drip-proof motors. From Table 2, it should be noted that the open drip-proof motors are limited to a maximum power of ~37 MWe. Therefore, for large scale plants such as NETL Baseline620 case, multiple barrel-type compressors, each fitted with a motor, are needed to handle the sCO_2 compression requirements.

Table 3. An example of calculation of sCO_2 power block equipment-only costs (x$1000) for a small scale 10 MW_e plant, and a large utility-scale Baseline620 case from Ref [10]

Component	10 MW_e Plant		NETL Baseline620 – 550 MW_e	
	(2017 $1,000)	% of total cost	(2017 $1,000)	% of total cost
NG-fired heater	$8,909	38.21%	-	
PC-fired heater	-		$216,300	45.91%
LTR	$2,056	8.82%	$81,860	17.37%
HTR	$3,324	14.25%	$40,150	8.52%
Direct dry cooler	$1,617	6.93%	$27,780	5.89%
Main compressor	$1,558	6.68%	$31,640	6.71%
Recompressor	$1,798	7.71%	$26,360	5.59%
Motors	$407	1.74%	$29,130	6.18%
Turbine	$2,831	12.14%	$13,160	2.79%
Generator	$471	2.02%	$4,756	1.00%
Gearbox	$340	1.46%	-	
Total equipment cost (2017 $1,000)	$23,310		$471,100	
Uncertainty range of total equipment cost	-28% to +35%		-27% to 35%	

For both examples in Table 3, the power turbine is assumed to be an axial turbine which generates the necessary electrical power to drive the compressor motors as well as other auxiliary plant equipment. For sizing and cost estimation of the direct dry sCO2 air cooler, the ambient temperature is assumed to be 30 °C and the tube bank has four tube rows and three passes.

The uncertainty range of the total equipment cost is calculated by propagating the uncertainties from individual components as described in Eq. (28).

$$U_{total} = \frac{\sum C_i . U_i}{\sum C_i} \quad (28)$$

where C_i is the equipment cost of individual component, U_i is the uncertainty associated with the individual component cost, and the summations occur over all components.

The component costs presented in Table 3 are equipment only cost and the necessary installation factors should be applied to calculate the bare erected cost (BEC) of the sCO_2 power block. The installation factor guidelines provided under each component section can be applied for calculating approximate BEC. Applying these installation factor guidelines to the 10 MW_e plant, the calculated total BEC of the sCO_2 power block is ~27.1M$ whereas the total equipment only cost is ~23.3M$ from Table 3. Further, it should be noted that CO_2 piping and inventory control costs are excluded from the above calculations, and can be expected to add another $1-2 million to the plant equipment cost.

Note that the costs in Table 3 for the 10 MW_e plant are not representative of the STEP facility, which is a first of a kind plant that will require additional costs for non-recurring engineering, site improvements, buildings, instrumentation and control systems, auxiliary electrical and mechanical systems, administrative overhead, contingencies, and operation & maintenance costs, among other expenses. Rather, this example is included in Table 3 to give a sense for the relative sCO_2 component costs that may be expected in such a plant.

The results of Table 3 roughly show that for the 10 MW_e plant, sCO_2 turbomachinery accounts for about 30% of the power block costs, recuperation and cooling accounting for another 30%, and the primary heater accounting for about 40%. For the large-scale plant, primary heater costs increase to about 45% of the total, with reduced turbomachinery costs (25%) and comparable recuperation and cooling costs (30%).

An alternative turbomachinery configuration for the 10 MW_e plant was also investigated to explore the cost tradeoffs. In the alternative configuration, both compressors are integrally-geared centrifugal machines driven by a single radial turbine, and the power turbine generates ~10 MW_e. The results yield a minimal 4% increase in the cost of the turbomachinery relative to the original turbomachinery configuration from Table 3. However, this example does not include the cost of sCO_2 piping, in which two additional high temperature pipe runs are needed for the compressor drive turbine.

The cost models proposed in this study are also used to update the sCO_2 equipment costs for a previous NETL study [10] and the updated results are compared to the costs calculated previously. Figure 8 presents this comparison for Baseline620 and Baseline760 cases from Ref [10]. The main difference between these two cases is the turbine inlet temperature of 620 °C for the Baseline620 case, and 760 °C for the Baseline760 case. The turbomachinery configuration for both the cases is the same as that described in the previous section. Also, since these are water-cooled plant designs, the recuperator cost scaling model was used to approximate the cost of the water/sCO_2 cooler. The primary heater costs are deliberately excluded from the comparisons since the NETL baseline cases from Ref [10] used oxy-fired circulating fluid bed (CFB) boiler as the primary heat source, whereas the primary heater cost algorithms proposed in the present work only included pulverized coal-fired and natural-gas fired primary heaters.

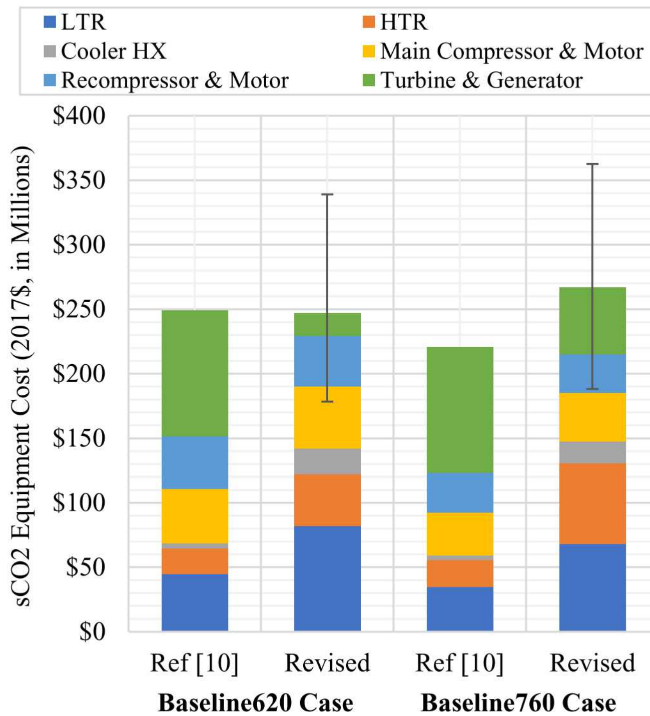

Figure 8. Comparison of sCO_2 equipment costs from previous NETL studies of Ref [10] with the current cost algorithms. Baseline620 and Baseline760 cases have turbine inlet temperatures of 620 °C and 760 °C, respectively.

Comparing the old and revised cost estimates in Figure 8, turbogenerator, recuperators, and cooler costs present noticeably large differences. Turbogenerator costs are significantly overpredicted by the old model, which was based on a rough estimate by Moullec [34], and did not include adjustments for high temperature material requirements. Recuperator and cooler costs are significantly underpredicted by the old model, in which heat duty was used as the scaling parameter. As noted previously, the recuperator and cooler costs scale better with UA rather than heat duty. The old and revised compressor cost algorithms predict similar costs for the sCO_2 compressors. Another noticeable difference is that going from Baseline620 to Baseline760 case, the old cost algorithms predict a decrease in the total equipment cost (excluding boiler and sCO_2 piping costs); whereas the revised cost algorithms predict a slight increase in the total equipment cost. Despite these differences, the old and revised estimates for the total equipment cost agree within the uncertainty bands of the revised estimates.

5 SUMMARY AND CONCLUSIONS

Compilation of sCO_2 component vendor quotes across multiple U.S. Department of Energy National Laboratories has allowed for the collaborative development of detailed, power law-based cost scaling relationships for coal- and natural gas-fired primary heaters, axial and radial turbines, centrifugal compressors, recuperators, and direct dry air coolers. The large number of vendor quotes available has also enabled the derivation of temperature correction factors to account for the cost increase associated with material upgrades as higher sCO_2 cycle temperatures are considered. Turbo-machinery costs have been broken down to include costs for motors, gearboxes, and generators, to allow cycle designers to explore the cost implications of various turbomachinery configurations. Further, through rigorous screening and vendor quote rating system, uncertainties on the developed cost scaling relationships have been quantified to enable propagation of sCO_2 power block cost uncertainties into the calculation of the COE for a given plant design. Component installation costs have also been surveyed, and recommended installation factors have been presented. Finally, application of the new cost models to two sCO_2 cycle design cases is presented to demonstrate their utility.

While a considerable number of vendor quotes and estimates have been considered in this study, there are several components for which the number of quotes available were insufficient to generate a suitable cost correlation. These include primary heaters for waste heat recovery, concentrated solar, and nuclear applications, water/sCO_2 coolers, turbine stop and control valves, and centrifugal pumps for condensed phase CO_2 cycle operation. Cost correlations for these components may be developed in future studies, though in the interim, rough cost correlations are given by Carlson for pumps and particle-based primary heat exchangers for CSP applications [16].

In addition, there are several cost correlations that would benefit from additional high-quality vendor quotes to reduce the uncertainty in the correlations, namely for radial turbines, integrally-geared compressors, and barrel-type compressors, although additional quotes would be beneficial for the axial turbines and primary heaters as well. Finally, additional vendor quotes may be sought to extend the range of validity of some of the above cost correlations. In particular, natural-gas primary heater costs should be extended to duties up to 100 MW_{th}, and gearbox costs are needed for larger shaft powers from 10-60 MW_{sh}. The recuperator cost scaling could be extended to include higher temperatures as needed for use in direct sCO_2 power cycles and may also benefit from the inclusion of a pressure drop cost scaling factor.

As construction commences on larger scale sCO_2 cycle demonstrations, additional component cost and installation information should become available to improve the cost models developed in this study. Nonetheless, the resulting component cost models from this study represent a significant improvement in the cost modeling capabilities available to sCO_2 cycle designers and analysts. In the near-term, this will allow for more accurate cost assessment of proposed sCO_2 cycles across the entire indirect sCO_2 temperature and size design space, including fossil, nuclear, CSP, and waste heat recovery applications from 5 to 750 MW_e in size. The long-term goal is that this capability will catalyze a shift from efficiency-based to economic-based sCO_2 cycle design and optimization. This will ultimately yield more economically competitive sCO_2 cycle designs and accelerate the commercialization of sCO_2 power cycle technology.

6 NOMENCLATURE

a	Cost model constant
b	Cost model power law exponent
c	Temperature correction factor constant
C	Component cost, 2017$
CR	Confidence rating
d	Temperature correction factor constant
f_T	Temperature correction factor
Q	Heat duty, MW_{th}
SP	Scaling Parameter
T_{bp}	Temperature correction factor breakpoint, °C
T_{max}	Maximum component temperature rating, °C
U	Uncertainty
UA	Conductance-area product, W/K
$\dot{V}$	Volumetric flow rate, m^3/s
$\dot{W}_e$	Electric power, MW_e
$\dot{W}_{sh}$	Shaft power, MW_{sh}

7 DISCLAIMERS

Sandia National Laboratories is a multimission laboratory managed and operated by National Technology and Engineering Solutions of Sandia, LLC., a wholly owned subsidiary of Honeywell International, Inc., for the U.S. Department of Energy's National Nuclear Security Administration under contract DE-NA-0003525.

8 ACKNOWLEDGEMENTS

The authors would like to thank Craig Turchi and Jared Fryar for their valuable contributions to the vendor database, Matt Carlson for providing a comprehensive example of sCO_2 component cost modeling in his 2017 paper [16], and Chuck White for his insights on NETL cost scaling practices. The authors would also like to acknowledge the support and encouragement of management from our respective laboratories, including Gary Rochau, Rich Dennis, and Travis Shultz.

9 REFERENCES

[1] S. A. Wright, R. F. Radel, M. E. Vernon, G. E. Rochau and P. S. Pickard, "Operation and Analysis of a Supercritical CO2 Brayton Cycle," Sandia National Laboratories, Albquerque, 2010.

[2] A. D. Akbari and S. M. Mahmoudi, "Thermoeconomic analysis & optimization of the combined supercritical CO2 (carbon dioxide) recompression Brayton/organic Rankine cycle," *Energy,* vol. 78, pp. 501-512, 2014.

[3] A. D. Akbari and S. M. Mahmoudi, "Thermoeconomic performance and optimization of a novel cogeneration system using carbon dioxide as working fluid," *Energy Conversion and Management,* vol. 145, pp. 265-277, 2017.

[4] X. Wang, Y. Wu, J. Wang, Y. Dai and D. Xie, "Thermo-Economic Analysis of a Recompression Supercritical CO2 Cycle Combined with a Transcritical CO2 Cycle," in *Proceedings of ASME Turbo Expo 2015*, Montreal, Canada, 2015.

[5] H. Zhao, Q. Deng, W. Huang and Z. Feng, "Thermodynamic and Economic Analysis and Multi-Objective Optimization of Supercritical CO2 Brayton Cycles," in *Proceedings of ASME Turbo Expo 2015*, Montréal, Canada, 2015.

[6] S. Hou, Y. Wu, Y. Zhou and L. Yu, "Performance analysis of the combined supercritical CO2 recompression and regenerative cycle used in waste heat recovery of marine gas turbine," *Energy Conversion and Management,* vol. 151, pp. 73-85, 2017.

[7] T. J. Held, J. Miller and D. J. Buckmaster, "A Comparative Study of Heat Rejection Systems for sCO2 Power Cycles," in *The 5th International Symposium - Supercritical CO2 Power Cycles*, San Antonio, Texas, 2016.

[8] S. R. Pidaparti, P. J. Hruska, A. Moisseytsev, J. J. Sienicki and D. Ranjan, "Technical and Economic Feasibility of Dry Air Cooling for the Supercritical CO2 Brayton Cycle using Existing Technology," in *The 5th International Symposium - Supercritical CO2 Power Cycles*, San Antonio, Texas, 2016.

[9] J. J. Sienicki, A. Moisseytsev and Q. Lv, "Dry Air Cooling and the sCO2 Brayton Cycle," in *Proceedings of ASME Turbo Expo 2017*, Charlotte, North Carolina, USA, 2017.

[10] C. White, D. Gray, J. Plunkett, W. Shelton, N. Weiland and T. Shultz, "Techno-economic Evaluation of Utility-Scale Power Plants Based on the Indirect sCO2 Brayton Cycle," National Energy Technology Laboratory, Pittsburgh, PA, 2017.

[11] C. W. White, W. W. Shelton, N. T. Weiland and T. R. Shultz, "sCO2 Cycle as an Efficiency Improvement Opportunity for Air-fired Coal Combustion," in *The 6th International Supercritical CO2 Power Cycles Symposium*, Pittsburgh, PA, 2018.

[12] T. J. Held, "Supercritical CO2 Cycles for Gas Turbine Combined Cycle Power Plants," in *Power Gen International*, Las Vegas, Nevada, 2015.

[13] Electric Power Research Institute, "High-Efficiency Thermal Integration of Closed Supercritical CO2 Brayton Power Cycles with Oxy-Fired Heaters," EPRI, Palo Alto, CA, 2018.

[14] S. A. Wright, C. S. Davidson and W. O. Scammell, "Thermo-Economic Analysis of Four sCO2 Waste Heat Recovery Power Systems," in *5th International sCO2 Power Cycles Symposium*, San Antonio, 2016.

[15] K. R. Zada, R. Kim, A. Wildberger and C. P. Schalansky, "Analysis of Supercritical CO2 Brayton Cycle Recuperative Heat Exchanger Size and Capital Cost with Variation of Layout Design," in *6th International Supercritical CO2 Power Cycles Symposium*, Pittsburgh, 2018.

[16] M. D. Carlson, B. M. Middleton and C. K. Ho, "Techno-Economic Comparison of Solar-Driven sCO2 Brayton Cycles using Component Cost Models Baselined with Vendor Data and Estimates," in *Proceedings of the ASME 2017 11th International Conference on Energy Sustainability*, Charlotte, North Carolina, USA, 2017.

[17] D. C. Miller, M. Syamlal, D. S. Mebane, C. Storlie, D. Bhattacharyya, N. V. Sahinidis, D. Agarwal, C. Tong, S. E. Zitney, A. Sarkar, X. Sun, S. Sundaresan, E. Ryan, D. Engel and C. Dale, "Carbon Capture Simulation Initiative: A Case Study in Multiscale Modeling and New Challenges," *Annual Review of Chemical and Biomolecular Engineering,* vol. 5, pp. 301-323, 2014.

[18] D. C. Miller, J. Siirola, D. Agarwal, A. P. Burgard, A. Lee, J. C. Eslick, B. Nicholson, C. Laird, L. T. Biegler, D. Bhattacharyya, N. V. Sahinidis, I. E. Grossmann, C. E. Gounaris and D. Gunter, "Next Generation Multi-Scale Process Systems Engineering Framework," *Computer Aided Chemical Engineering,* vol. 44, pp. 2209-2214, 2018.

[19] S. Jenkins, "CEPCI Updates: January 2018 (Prelim.) and December 2017 (Final)," Chemical Engineering, 19 March 2018. [Online]. Available: https://www.chemengonline.com/cepci-updates-january-2018-prelim-and-december-2017-final/?printmode=1. [Accessed 10 September 2018].

[20] National Energy Technology Laboratory (NETL), "Quality Guidelines for Energy System Studies, Cost Estimation Methodology for NETL Assessments of Power Plant Performance," NETL, Pittsburgh, January 2013.

[21] D. Fleming, T. Holschuh, T. Conboy, G. Rochau and R. Fuller, "Scaling Considerations for a Multi-Megawatt Class Supercritical CO2 Brayton Cycle and Path Forward for Commercialization," in *Proceedings of ASME Turbo Expo 2012, GT2012-68484*, Copenhagen, Denmark, 2012.

[22] J. Noall, "Selection of Turbine Type for s-CO2 Applications," in *Supercritical CO2 Power Cycles Symposium*, San Antonio, Texas, 2016.

[23] E. W. Lemmon, M. L. Huber and M. O. McLinden, "NIST Standard Reference Database 23: Reference Fluid Thermodynamic and Transport Properties-REFPROP, Version 9.1, National Institute of Standards and Technology," National Institute of Standards and Technology, Gaithersburg, 2013.

[24] AACE International Recommended Practice Number 16R-90, "Conducting Technical and Economic Evaluations -- As Applied for the Process and Utility Industries; TCM Framework 7.3 -- Cost Estimating and Budgeting," AACE, 2003.

[25] H. W. Coleman and W. G. Steele, Experimentation, Validation, and Uncertainty Analysis for Engineers, Hoboken: John Wiley & Sons, Inc., 2009.

[26] M. Mecheri, "sCO2 Closed Brayton Cycle for Coal-Fired Power Plant: an Economic Analysis of a Technical Optimization," in *2nd European Supercritical CO2 Conference*, Essen, Germany, 2018.

[27] National Energy Technology Laboratory (NETL), "Cost and Performance Baseline for Fossil Energy Plants Volume 1a: Bituminous Coal (PC) and Natural Gas to Electricity, Revision 3," NETL, Pittsburgh, July 2015.

[28] National Energy Technology Laboratory (NETL), "Quality Guidelines for Energy System Studies -- Capital Cost Scaling Methodology," NETL, Pittsburgh, January 2013.

[29] A. C. Caputo, M. Palumbo, P. M. Pelagagge and F. Scacchia, "Economics of biomass energy utilization in combustion and gasification plants: effects of logistic variables," *Biomass and Bioenergy,* vol. 28, pp. 35-51, 2005.

[30] H. A. Navarro and L. C. Cabezas-Gómez, "Effectiveness-NTU computation with a mathematical model for cross-flow heat exchangers," *Brazilian Journal of Chemical Engineering,* vol. 24, no. 4, pp. 509-521, 2007.

[31] "Aspen Icarus Reference Guide: Icarus Evaluation Engine (IEE)," 2012.

[32] M. Walker, A. Kruizenga, P. Weck, E. Withey and D. Fleming, "Progress in Overcoming Materials Challenges with S-CO2 RCBCs: Final Report," Sandia National Laboratories, Albuquerque, 2016.

[33] S. E. Zitney and E. A. Liese, "Dynamic Modeling and Simulation of a 10 MWe Supercritical CO2 Recompression Closed Brayton Power Cycle for Off-Design, Part-Load, and Control Analysis," in *The 6th International Supercritical CO2 Power Cycles Symposium*, Pittsburgh, 2018.

[34] Y. L. Moullec, "Conceptual study of a high efficiency coal-fired power plant with CO2 capture using a supercritical CO2 Brayton cycle," *Energy,* vol. 49, pp. 32-46, 2013.

10 ANNEX A

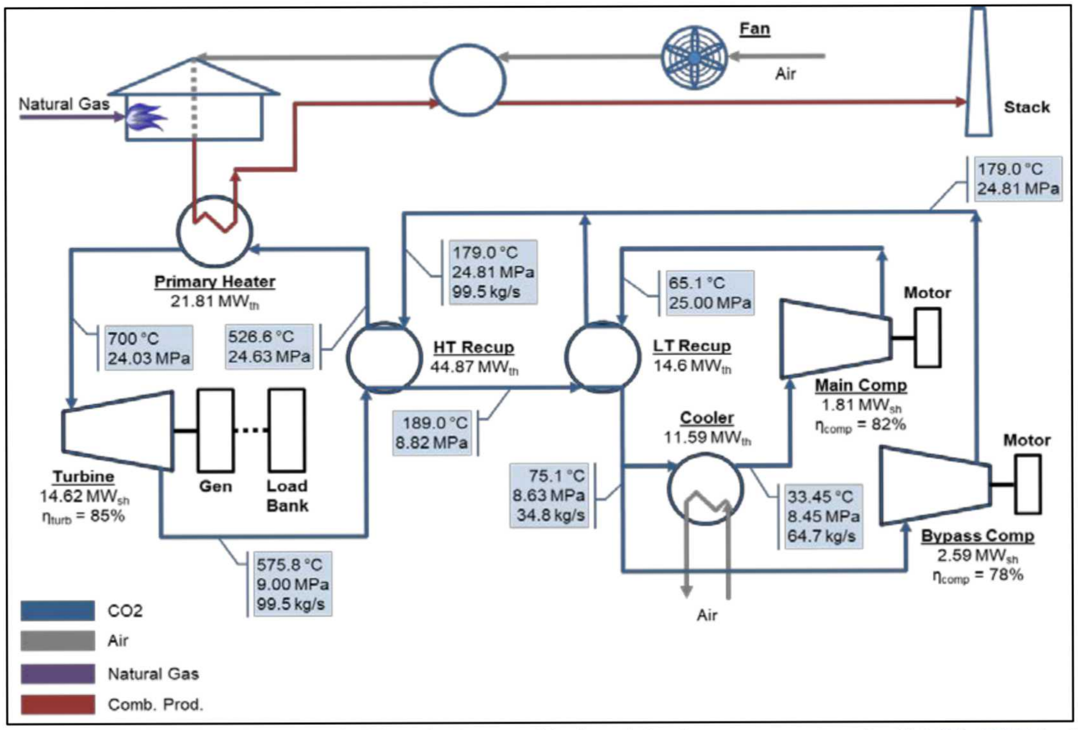

Figure 9. Simplified block flow diagram of sCO_2 RCBC power block and the design state points for 10 MWe STEP facility